Strong Suppression of Impurity Accumulation in Steady-State Hydrogen Discharges with High Power NBI Heating on LHD

Y. Nakamura[1, 2], N. Tamura[1], M. Yoshinuma[1, 2], C. Suzuki[1], S. Yoshimura[1], M. Kobayashi[1, 2], M. Yokoyama[1, 2], M. Nakata[1], K. Nagaoka[1], K. Tanaka[1], B. J. Peterson[1, 2], K. Ida[1, 2], M. Osakabe[1, 2], T. Morisaki[1, 2] and the LHD Experiment Group

[1] National Institute for Fusion Science, National Institutes of Natural Sciences, Toki, Japan
[2] SOKENDAI (Graduate School for Advanced Studies), Toki, Japan

E-mail: nakamura.yukio@nifs.ac.jp

Abstract. Strong suppression of impurity accumulation is observed in long pulse hydrogen discharges with high power NBI (Neutral Beam Injection) heating (P_{nbi} > 10 MW) on the Large Helical Device (LHD), even in impurity accumulation window where the intrinsic impurities such as Fe and C are always accumulated into the plasma core. Density scan experiments in these discharges demonstrate a new operational regime without impurity accumulation in steady state hydrogen discharges. Impurity pinch decreases with increasing ion temperature gradient and carbon Mach number. The peaking of the measured carbon profiles shows strong anti-correlations with the Mach number and its radial gradient. An external torque has a big impact on impurity transport and strong co-current rotation leads to an extremely hollow carbon profile, so-called 'impurity hole' observed in high ion temperature modes. Impurity pinch in the plasmas with net zero torque input (balanced NBI injection) is also strongly reduced by increasing ion temperature gradient, which can drive turbulent modes. The combination effect of turbulence and toroidal rotation plays an important role in the impurity transport.

1. Introduction

Impurity transport study in tokamak and stellarator plasmas has been an issue of concern for several decades. Central accumulation of impurities produces a deleterious combination of fuel dilution and radiation, which strongly limits the possibility of achieving practical fusion energy, and an uncontrolled impurity accumulation may even terminate the fusion plasma. Understanding impurity transport is crucial for sustaining high performance plasmas in magnetic confinement devices.

In heliotrons and stellarators, large superconducting devices such as LHD [1] and W7-X (Wendelstein 7-X) [2] already comply with long-pulse operation and focus upon the establishment of high performance steady-state plasmas. Significant progress has been already made in sustaining high temperature plasma and maintaining the integrity of the machine for long time in LHD [3-5]. One-hour discharge with the high temperature plasma of 2 keV has been achieved with ICH and ECH heating power of 1.2 MW. The energy injected into the plasma amounts to 3.4 GJ [5]. In steady state operation, one of critical issues is to avoid impurity accumulation, which can lead to early pulse termination by radiation collapse. Long pulse discharges with ICH were usually conducted in the scheme of hydrogen minority heating and helium dominant plasmas were sustained by controlling the minority ratio. Most of long pulse discharges with ICH were terminated by radiation collapse due to the increase of plasma density or the penetration of impurity flakes into the plasma [6]. However, there has never been an event of long-term impurity accumulation. On the other hand, long pulse hydrogen discharges with NBI heating showed impurity accumulation behavior for high-Z impurities. This notable result might be attributed to the difference between helium and hydrogen plasmas, i.e. the change of impurity transport due to background ions [7]. For hydrogen discharges, the intrinsic impurities such as Fe and C were accumulated in a specific range of impurity collision frequency, which is so-called 'impurity accumulation window' [8]. Impurity transport study by using active impurity pellet injection indicated a long impurity confinement time in this window [9, 10]. Such an impurity behavior was also observed in

other helical devices and a better understanding of impurity transport was obtained from the inter-machine comparison [11]. Recently, study on impurity shielding criteria for LHD steady-state hydrogen plasmas revealed the important role of radial electric field and the impurity screening effect in the ergodic layer [12]. Theoretical predictions based on neoclassical transport theory for non-axisymmetric configurations underline the importance of radial electric field. In the standard case with negative radial electric field, the so-called ion-root regime, high-Z impurities are drawn toward the center. Only in the low-density regime, it is possible to establish the electron root with positive radial electric field, which flushes out impurities. On the other hand, impurity transport studies in the scrape-off-layer (SOL) region demonstrated a favorable impact on the impurity screening, i.e. the screening of impurity influx from the divertor plates [13, 14]. Impurity transport simulations indicated a clear physical picture of impurity screening in the SOL [15, 16]. The cross-field heat conduction governs the ion energy transport across the islands under high density, low temperature conditions. The friction force dominates over the ion thermal force, dragging impurities outwards. Besides, in short pulse discharges, high confinement plasmas with a high ion temperature at low collisionality indicated an extremely hollow profile of impurity, which is so called 'impurity hole' [17-19]. The radial electric field in the core region is weak negative [20] and clear physical basis on the strong outward convection is not yet found. Turbulent transport is another important contribution to impurity transport and might gain increasing importance in impurity transport for tokamak plasmas, but there is no clear evidence in experimental observation and also in theoretical analysis including simulation studies for non-axisymmetric configurations.

In this paper, the operational regime in steady-state discharge will be extended to high temperature and high density region by increasing NBI heating power and explored favorable scenarios capable of preventing impurity accumulation. Impurity behavior in steady state hydrogen discharges with high power heating will be described in section 2, presenting a new operational regime without impurity accumulation. The parameter dependences of carbon density profile will be investigated and the correlation with ion temperature gradient and toroidal rotation will be described. In section 3, the impact of NBI torque input on impurity transport will be investigated and the profile structure of carbon density is compared with that in high ion temperature mode, followed by a description of impurity transport in net zero torque input discharges in section 4. A general discussion and comprehensive understanding of impurity transport in LHD will be also discussed in section 5.

2. Impurity behavior in steady-state hydrogen discharge

Several specific features of impurity behavior have so far been found in LHD, which has a fully superconducting magnet and generates a heliotron magnetic configuration (l/m =2/10) in steady state for plasma confinement. Steady-state hydrogen discharges have been produced with a constant heating power and maintained with a constant electron density for more than 5 seconds. Density scans of long pulse discharges showed intrinsic impurity accumulation in a specific density range (plasma collisionality), which is called the 'impurity accumulation window'. Such an accumulation window has always been found at anywhere in the density scan for the discharges with NBI heating power of less than 10 MW. Recently, higher NBI heating power (P_{nbi} > 10 MW) is available to long pulse operation in LHD and impurity behavior in high temperature regime is investigated in the magnetic configuration with the major radius R = 3.6 m.

2.1. Suppression of impurity accumulation in high power NBI discharge

In this experimental series, the combined tangential NBI heating power with co-injection and counter-injection with respect to the direction of toroidal magnetic field (B_t = -2.75 T) is employed. The perpendicular NBI heating power is added to measure carbon density profile by a charge exchange spectroscopy (CXS). Figure 1 shows typical long pulse discharges with different heating power. In the case of low power heating (P_{nbi} = 9.5 MW), the plasma central electron temperature (T_{e0}) extremely decreases with time. The radiated power density (S_{rad}) increases in the core region and the impurity line emission (Fe XXIII) strongly brightens in the plasma core because of the stainless steel plasma chamber wall. The carbon from graphite divertor tiles is accumulated into the core plasma. In contrast, all the plasma parameters are maintained almost constant in the high power discharge (P_{nbi} = 13 MW) and the amount of intrinsic impurities (Fe, C) in the plasma remains constant during the discharge. The impurity accumulation behavior as seen in the low power case is strongly suppressed. Figure 2 shows the radial profiles of electron temperature, radiated power density and carbon density in the last stage of the discharge (t ~ 6.5 s). For the low power discharge, the electron temperature is markedly reduced in the core region. The radiated power increases largely in the core plasma and the radiation profile becomes peaked with time. This remarkable increase in core radiation is caused by intrinsic metallic impurities (mainly iron), thereby resulting in flattening the temperature profile. The carbon density also increases in the core region and a remarkable peaking is observed in the carbon profile. In contrast, a peaked profile of electron temperature is maintained during the discharge in the high power case. The radiation profile with a hollow shape is maintained until the end of the discharge. The increase of core carbon density is stopped at around 1 s after the injection of high power NBI and the carbon profile with a flat shape is maintained during the discharge.

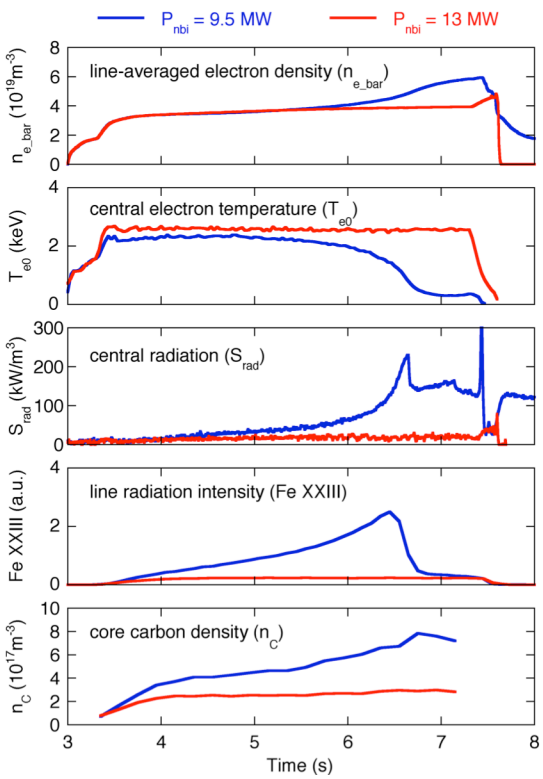

FIG. 1. Typical long pulse discharges with low (P_{nbi} = 9.5 MW) and high power (P_{nbi} = 13 MW) NBI heating. Strong suppression of impurity accumulation is observed in the long pulse discharge with the high power heating.

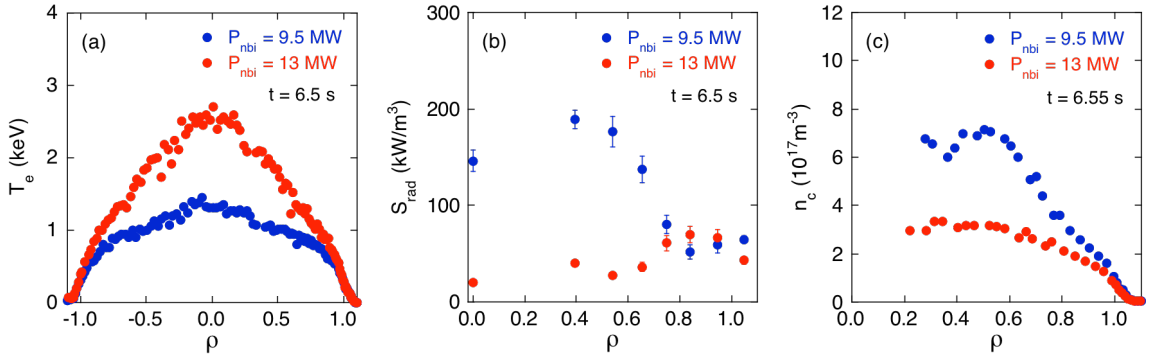

FIG. 2. Radiation profiles of (a) electron temperature, (b) radiated power density and (c) carbon density at t ~ 6.5 s in the discharges with different heating power of 9.5 and 13 MW.

Thus, strong suppression of impurity accumulation is found in steady-state hydrogen discharges with higher NBI heating power more than 10 MW.

Density scan experiments show that there is no impurity accumulation in the high power discharges. Figure 3 shows the dependence of the increasing rate of core carbon density (dn_c/dt) on background ion collisionality. In the case of low power heating (P_{nbi} = 7.5 MW), the core carbon density remarkably increases with time in a specific collisionality region (impurity accumulation window) as observed before. However, in the discharges with high power heating (P_{nbi} = 13 MW), the core carbon density remains almost constant during the discharge and impurity accumulation behavior does not appear in the overall collisionality range. This means that a new operational regime without impurity accumulation is found in steady state hydrogen discharges on LHD.

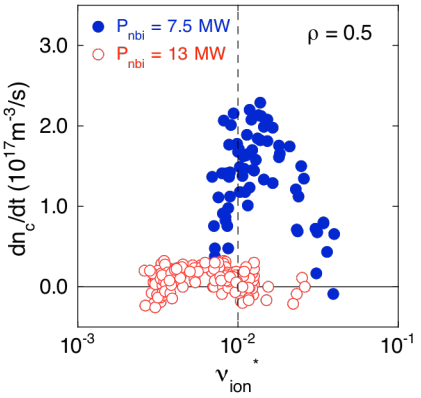

FIG. 3. Dependence of the increasing rate of core carbon density on background ion collisionality at ρ = 0.5 for different NBI heating power. The impurity accumulation window observed in the low power operational regime disappears in the high power discharges.

2.2. Mapping of impurity behavior on n-T space

Impurity behavior in long pulse hydrogen discharges with NBI heating can be classified with the plasma parameters (n, T : electron density and temperature) at the plasma edge as shown in Fig. 4. The evaluation criterion for impurity accumulation is based on the increase of core radiation ($dS_{rad}/dt > 0$). There is no significant change of core radiation in the discharges without impurity accumulation. Physical studies on the critical condition at either side of impurity accumulation window provide two different physical pictures based on neoclassical impurity transport in the core plasma and on classical theory in the SOL region [12]. Impurity behavior is generally dominated by the radial electric field (E_r) and impurity accumulation is always observed in the ion root with a large negative E_r (closed blue points). The dashed line is expressed by the constant ion collisionality with the same E_r value. Below the solid line, intrinsic impurities are shielded by friction force in the ergodic layer. The open red points indicate recent high power NBI discharges and impurity accumulation does not appear even in the region between two boundaries where impurity accumulation was expected. This suggests that there exists no impurity accumulation in high performance plasmas with high power heating (P_{nbi} > 10 MW) and

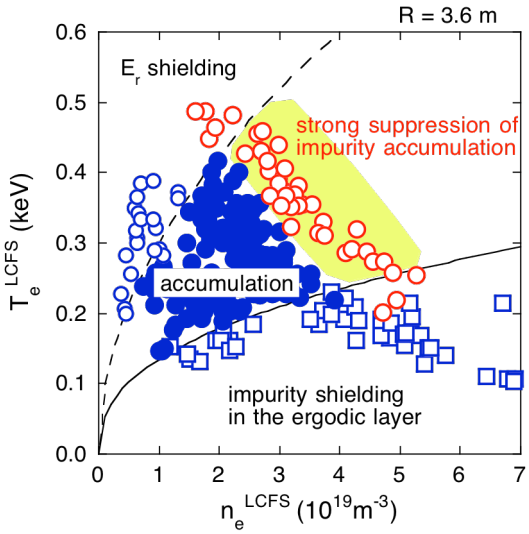

FIG. 4. n-T diagram at the plasma edge for impurity behavior in hydrogen discharges with R = 3.6 m. The closed and open blue symbols indicate the discharges (P_{nbi} < 10 MW) with and without impurity accumulation, respectively. The dashed and solid lines indicate the critical conditions at either side of impurity accumulation window. The open red points represent the discharges with the strong suppression of impurity accumulation (P_{nbi} = 13 MW).

it is excellent for realizing fusion plasmas.

2.3. Transition to stationary state without impurity accumulation

The plasmas in the region indicated by the yellow (Fig. 4) have a large negative E_r as well as that in low power discharges. A new contribution to impurity transport is required to explain the strong suppression of impurity accumulation. In order to keep the E_r contribution (neoclassical one) constant, the specific discharges with constant ion collisionality are selected from those with various heating powers, because the ion collisionality is a good predictor of E_r. Figure 5 shows the dependences of carbon density increasing rate (dn_c/dt) on normalized ion temperature gradient ($R/L_{Ti} = -(R/T_i)dT_i/dr$) and carbon Mach number in hydrogen plasmas with the constant ion collisionality ($\nu_{ion}^* \sim 0.01$) at $\rho = 0.5$, in which impurity accumulation appears remarkably as shown in Fig. 3. In this case, the strength of impurity pinch is estimated by the time derivative of carbon density at the middle of minor radius ($\rho = 0.5$). When the temperature gradient is increased with the heating power, the increasing rate of carbon density (impurity pinch) decreases up to zero and then remains at nearly zero level, that is, stationary state without impurity accumulation (Fig. 5(a)). A similar correlation is also observed between impurity pinch and carbon Mach number (Fig. 5(b)). These relationships cannot be explained only by neoclassical impurity transport, which is dominated by the E_r contribution.

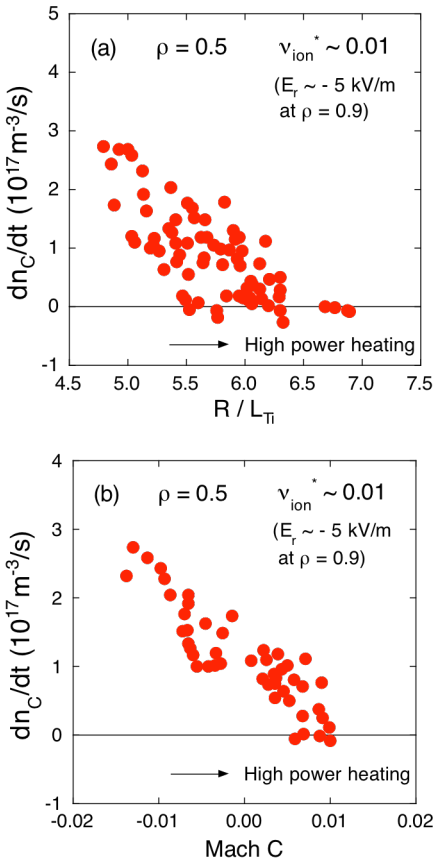

FIG. 5. Dependences of impurity pinch on (a) normalized ion temperature gradient (R/L_{Ti}) and (b) carbon Mach number (Mach C) under the constant ion collisionality condition. The impurity pinch is estimated by the increasing rate of carbon density (dn_c/dt) at $\rho = 0.5$. In these discharges, the E_r at $\rho = 0.9$ is negative and around - 5 kV/m.

2.4. Parameter dependence of carbon density profile

In order to make clear a new contribution to impurity transport, a database of carbon density

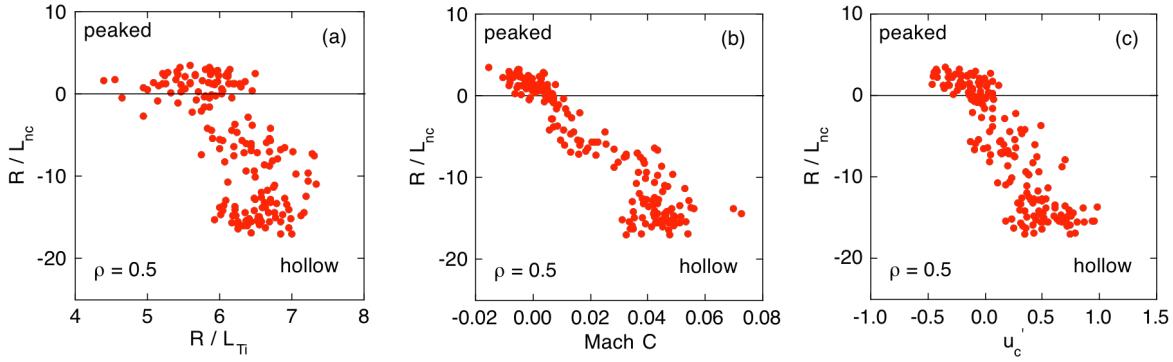

FIG. 6. Correlations in the high power NBI discharge database of carbon density measurements at $\rho = 0.5$. The normalized carbon density gradients (R/L_{nc}) are plotted as a function of (a) normalized ion temperature (R/L_{Ti}), (b) carbon Mach number (Mach C) and (c) normalized toroidal rotation gradient (u_c'). The positive (negative) value of R/L_{nc} indicates a peaked (hollow) carbon density profile.

profile from steady-state discharges with high power NBI heating has been constructed. All shots have a continuous 13 MW NBI heating power from the beams, which consist of tangential beams (co-injection: 6.3 MW, counter-injection: 3 MW) and perpendicular beams (3.7 MW). These discharges are produced with the magnetic axis R = 3.6 m and with the toroidal field B_t = -2.75 T. The database covers a range of plasmas with averaged electron densities between 1.5 and 5 x 10^{19}m^{-3}. A number of strong correlations are visible in the database (Fig. 6). The most striking is between the Mach number $u_c = v_{tor}/v_{th}$ and the carbon density gradient $R/L_{nc} = (R/n_c)dn_c/dr$ (Fig. 6(b)). The carbon density profile becomes hollow with increasing the Mach number. A similar strong correlation can also be seen between R/L_{nc} and the rotation gradient $u_c' = -(R/v_{th})dv_{tor}/dr$ (Fig. 6(c)). The similarity between figures 6(b) and 6(c) is due to a high correlation between u_c and u_c', which is a consequence of peaked toroidal rotation profiles that result from central NBI heating. Since temperature gradients are the primary quantity in determining the characteristics of turbulent modes, the correlations between R/L_{Ti} and R/L_{nc} provide a strong signature that turbulence is important in the impurity transport.

3. Impact of NBI torque input on impurity transport

Steady-state discharges have so far been conducted with almost constant NBI heating power, i.e. constant NBI torque input. The toroidal velocity depends on the plasma density and increases with decreasing the density [20]. Here, the effect of external torque on impurity transport is investigated by changing the NBI torque input in low collisionality region. Figure 7 shows the change of impurity transport by switching the NBI heating from co-injected beam to counter-injected beam. In this discharge, the plasma is produced by ECH and the co-NBI is injected from 3.3 s to 4.8 s. Then the counter-NBI is injected from 4.8 s to 6.3 s. The perpendicular-NBI is added to use for the CXS measurements. The central temperatures (T_e and T_i) and temperature gradients (R/L_{Te} and R/L_{Ti} at ρ = 0.5) do not largely change at the switching time (t = 4.8 s). In contrast, a remarkable change of core carbon density n_c and carbon density gradient R/L_{nc} (ρ = 0.5) is observed with changing the toroidal velocity V_t and rotation gradient u_c' (ρ = 0.5). The carbon density profile becomes hollow in the last stage of co-injection and a strong peaking of carbon density is observed in the counter injection phase, as shown in Fig. 8(a). The carbon

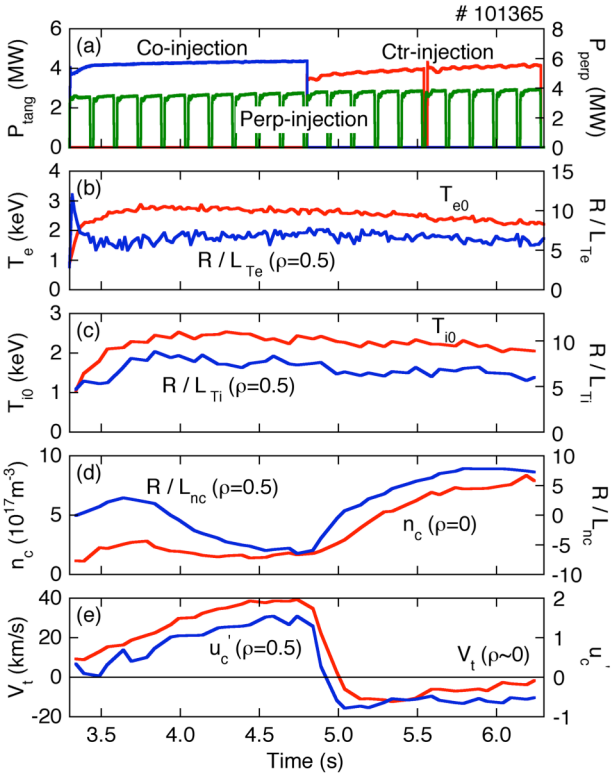

FIG. 7. Change of impurity transport by switching the NBI torque input from co-injection to counter-injection at t = 4.8 s. Time evolutions of (a) tangential and perpendicular NBI power, (b) central electron temperature T_{e0} and normalized radial gradient R/L_{Te} (ρ = 0.5), (c) central ion temperature T_{i0} and its radial gradient R/L_{Ti} (ρ = 0.5), (d) central carbon density n_c and normalized radial gradient R/L_{nc} (ρ = 0.5) and (e) central toroidal rotation velocity V_t (ρ ~ 0) and its radial gradient u_c' (ρ = 0.5) are indicated. This hydrogen discharge is produced with the magnetic axis R = 3.6 m and with the toroidal field B_t = -2.75 T.

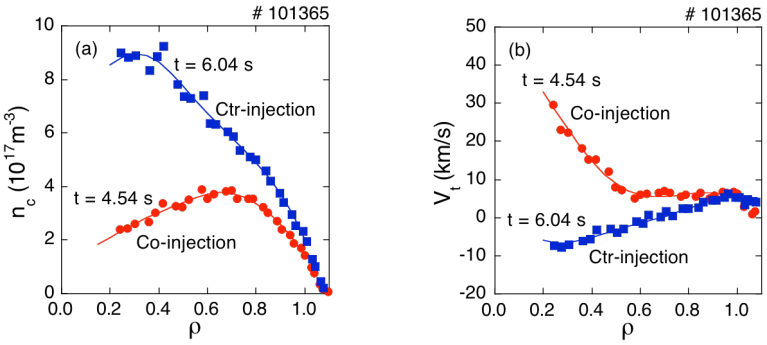

FIG. 8. Radial profiles of (a) carbon density and (b) toroidal rotation velocity at the co-injection (t = 4.54 s) and counter-injection (t = 6.04 s) phase in the discharge # 101365.

toroidal velocity in the core region increases with time in the phase of co-injection and abruptly changes to inverse velocity (Fig. 8(b)) after the counter-injection. The rotation gradient indicates the same behavior as the toroidal velocity. This drastic response of carbon density profile to NBI torque input suggests that an external torque input has a big impact on impurity transport.

Studies on parameter dependence of carbon density profile show a deep understanding of external torque input effect. Figure 9 shows the dependence of carbon density gradient on NBI torque input, which is normalized by the average electron density. All data points are estimated at around 1 s after the injection of directed NBI. The NBI beams consist of two co-current beams, one counter beam and two perpendicular beams. The directed NBI power P_d is calculated by subtracting counter-injection NBI power P_{ctr} from co-injection one P_{co}. The single NBI denotes each directed tangential beam alone and the mixed NBI the combined beams. Consequently, the total power with mixed NBI is larger than that with the single NBI. In the discharges with counter-NBI injection, the carbon profile becomes peaked and the density gradient at ρ = 0.5 has a positive value. The carbon density gradient decreases with increasing the NBI torque input and an extremely hollow profile of carbon density (R/L_{nc} ~ -25) is observed in the combined co-NBI injection with a large torque input. Such a strong hollow profile is comparable to that of 'impurity hole', which is found in high ion temperature modes [17-19]. It is worth noting that the impurity hole can be produced even in standard confinement regime.

In this experimental series where the NBI torque input is mainly changed, a database of carbon density profiles has also been constructed. Figure 10 shows the correlations between the carbon density gradient and various plasma parameters (ion temperature gradient, carbon Mach number and toroidal velocity gradient). One can see several strong correlations in this database. The well-regulated correlation is observed between the Mach number and the carbon density gradient (Fig. 10(b)) and the hollowness of carbon density increases with the Mach number. The carbon Mach number extends up to 0.2, which is around five times in comparison with that in the steady state discharges (Fig. 6(b)). A similar correlation is

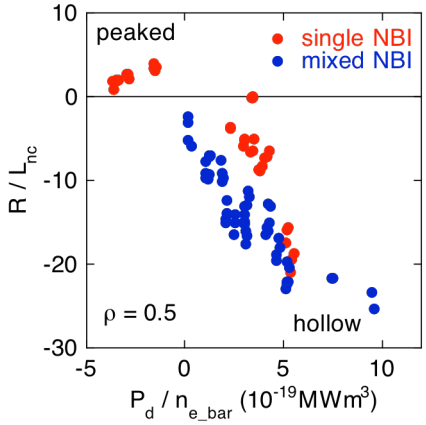

FIG. 9. Dependence of normalized carbon density gradient on NBI torque input. The NBI torque input is estimated by a directed tangential NBI power P_d (= P_{co} - P_{ctr}) normalized with averaged electron density n_{e_bar}. The single and mixed NBI denote each directed beam alone and combined beams, respectively.

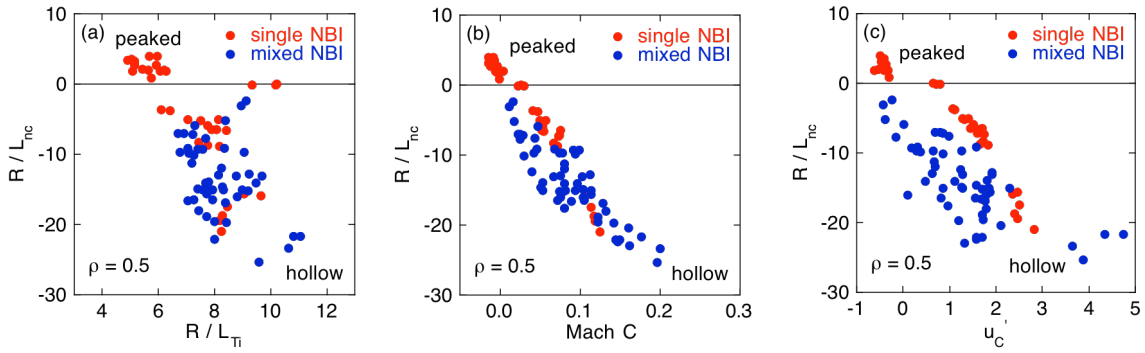

FIG. 10. Correlations in NBI torque input discharge database of carbon density measurements at ρ = 0.5. The normalized carbon density gradients are plotted as a function of (a) normalized ion temperature, (b) carbon Mach number and (c) normalized toroidal velocity gradient.

also observed between R/L_{nc} and the toroidal velocity gradient (Fig. 10(c)), but contains two branches due to different total NBI heating powers. The carbon density profiles in higher power discharges with mixed NBI become deeply hollow in comparison with those in lower power discharges with single NBI. The carbon density gradient has a significant decreasing trend with increasing the ion temperature gradient. However, there exits some points deviating certainly from the main trend and they have a minimum value of temperature ratio ($T_e/T_i \sim 1.0$), which leads to the reduction of the growth rate of turbulence. Clearly, the toroidal velocity (Mach number) has correlation with the NBI torque input and the independent variables plotted on the x-axes also have correlations between them (e.g. NBI torque inputs, temperature gradients and rotation): a strong correlation between rotation and ion temperature gradient (not shown) is present.

The primary correlation, between rotation (rotation gradient) and impurity peaking is not caused by a single mechanism, but is a non-trivial combination of the correlations between NBI torque inputs, temperature gradients, and rotation. These quantities together determine the impurity transport characteristics in such a way that the overall result produces the strong correlation shown here.

4. Effect of ion temperature gradient on impurity transport in net zero torque discharge

In order to distinguish the effect of ion temperature gradient on impurity transport, the discharges with net zero torque input (balanced NBI injection) have been selected and the parameter dependences of carbon density profile are investigated. The balanced NBI injections with co-injection and counter-injection beams have only a very small torque input ($-0.3 < P_d/n_{e\_bar} < 0.3$), which has no influence on impurity transport. The perpendicular NBI beam with the energy of 44 keV is added to increase the ion temperature. The carbon Mach number ranges from -0.015 to 0.01 and the rotation gradient from -0.6 to 0.1. There is no significant correlation between R/L_{nc} and these parameters. However, a distinct correlation is found between R/L_{nc} and ion temperature gradient as shown in Fig. 11, where all data points are estimated at around 1 s after the balanced NBI injection. The

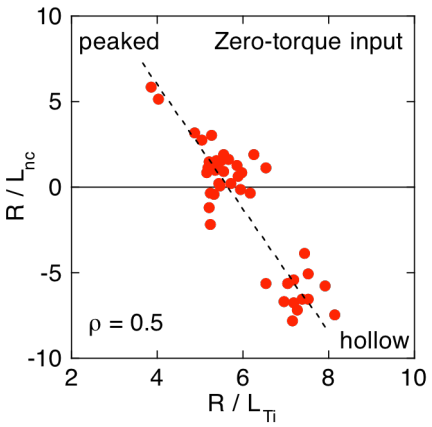

FIG. 11. Dependence of carbon density gradient on ion temperature gradient at ρ = 0.5 in the discharge with net zero torque input. In these discharges, the toroidal rotation velocity is very small.

carbon density profile becomes hollow with increasing the ion temperature gradient. This suggests that the ion temperature gradient contributes to the strong outward convection in impurity transport and turbulence is important in the impurity transport.

5. Discussions

As indicated in n-T diagram for impurity behavior (Fig. 4), impurity accumulation behavior is basically dominated by neoclassical impurity transport, which strongly depends on the radial electric field (E_r), in the plasmas with relatively low power heating. The E_r at the plasma edge is always negative in the impurity accumulation window and the negative E_r values remain even in high power discharges. Here, in order to investigate the neoclassical contribution to impurity transport, the neoclassical impurity flux in high power discharges is calculated by DKES/PENTA code [21]. This allowed the earlier transport coefficients based on the DKES model to be used and momentum conservation to be achieved at least at a fluid moment level. These approaches were extended to include impurities and incorporated into computational models. Figure 12 shows a simulation result for stationary plasma in high power discharges without impurity accumulation. In this case, there is still no external torque input in the momentum transport equation. The temperatures and densities of multi-species (electron, ion, helium and carbon) are given by fitting the profiles measured in the discharge (# 121260). The simulation results show that the E_r is negative and the carbon impurity flux is inward in a whole region of plasma, which results in carbon impurity accumulation. This is in contradiction with the experimental results in high power discharges and the strong suppression of impurity accumulation cannot be explained by neoclassical theory without an external torque input.

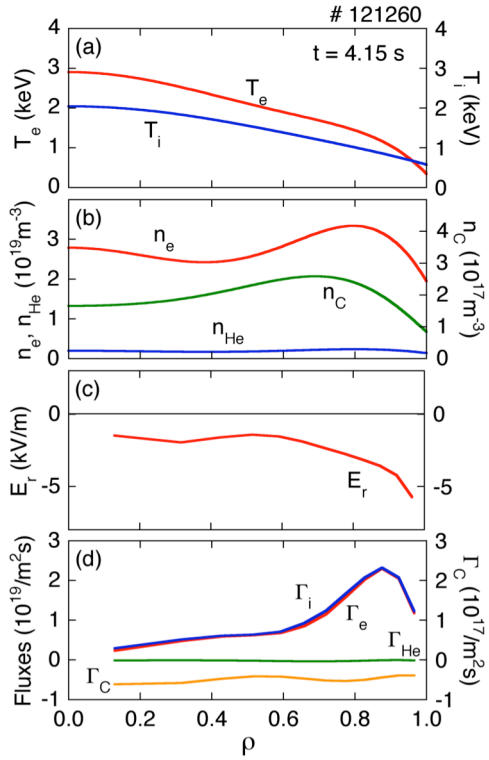

FIG. 12 Neoclassical simulation with the DKES/PENTA code for stationary plasma in high power discharges. Radial profiles of (a) plasma temperatures (T_e, T_i), (b) particle densities (n_e, n_{He}, n_C), (c) radial electric field and (d) particle fluxes (Γ_e, Γ_i, Γ_{He}, Γ_C) are indicated.

In steady state discharges with relatively low power heating, the NBI torque input is not so large and the rotation velocity is so small even at the middle of minor radius because the rotation velocity strongly decreases with increasing the plasma density in the outer region ($\rho > 0.5$) due to parallel viscosity [20]. When the heating power increases largely, significant rotation velocity appears even at $\rho = 0.5$ (Fig. 5(b) and Fig. 6(b)) and the impact of external torque input on impurity transport can be seen clearly in the plasmas with relatively low collisionality as described in section 3. One of possible candidates for the suppression of impurity accumulation is the modification of neoclassical impurity transport due to external torque input. The effect of NBI momentum input on neoclassical transport has been reported for tokamak plasmas in several papers [22, 23], although there is no calculation or simulation result for helical plasmas. Radial impurity transport fluxes are produced by the direct momentum exchange between injected beam particles and impurities or the radial electric field obtained from momentum balance. These impurity fluxes depend on the directions of beam, toroidal field and plasma current and tend to cancel each other out. Moreover, an

inertial effect produced by the beam-induced plasma rotation produces a radial impurity transport flux. The drastic (nonlinear) modification of neoclassical fluxes would be expected if Mach-one conditions are approached or exceeded. Since the carbon Mach number is less than 0.2 in our experiments, it is difficult to explain a strong hollow profile (outward convection) observed in the carbon density profile.

Another probable candidate for suppressing impurity accumulation is turbulent impurity transport including toroidal rotation effect. Since the strong connections between particle and toroidal momentum transport are presented, the turbulent impurity transport is also affected by toroidal rotation through momentum transport. The impact of the toroidal rotation and its radial gradient can become important for impurities due to heavier mass and lower thermal velocity (larger Mach number) [24-27]. The turbulent impurity flux is expressed by $\Gamma_z = n_z D_z (R/L_{nz} + C_T R/L_{Tz} + C_u u_z' + C_p)$, where in addition to diagonal diffusion R/L_{nz}, thermodiffusion $C_T R/L_{Tz}$ and pure convection C_p, an additional off-diagonal contribution $C_u u_z'$ is presented, proportional to the gradient of the toroidal velocity. The experimental impurity behaviors in the ASDEX upgraded tokamak have been well reproduced by the theoretical modeling, which is due to a combination of the turbulent regime and an impurity flux by rotation gradient [25, 26]. In the cases with dominant ITG modes, both of thermodiffusion term and roto-diffusion term due to toroidal rotation are directed outward. The peaking of boron profile is reduced with increasing rotation velocity (the boron Mach number) and its radial gradient. In our experimental databases, ITG modes can be driven in high temperature plasmas with $R/L_{Ti} > 5$ [27] and the decrease in carbon peaking with increasing the carbon Mach number is qualitatively consistent with the theoretical prediction.

In LHD, a strong hollow profile of impurities, the so-called ‘impurity hole’, has been observed in high ion temperature modes. In these discharges, a large toroidal rotation is always accompanied with the high ion temperature gradient in the core plasma. Certainly, the ion temperature gradient has an affect on impurity transport and the carbon profile becomes hollow with increasing the temperature gradient as observed in the discharges with net zero torque input (Fig. 11). However, the strong correlation between R/L_{nc} and the Mach number in our results indicates that the toroidal rotation also plays an important role in the impurity transport.

At last, in fusion devices, it is difficult to keep a large external torque input and stationary operation at low or zero injected torque is essential. As for the problems to be solved, it can be pointed out that spontaneous rotation observed in LHD [28] is a key issue and the effect of intrinsic toroidal rotation on impurity transport should be investigated in future.

6. Summary

Steady state discharges in LHD have been conducted with higher NBI heating power ($P_{nbi} > 10$ MW) and the operational regime was extended to high temperature and high density region. Impurity behavior has been investigated to explore favorable scenarios without impurity accumulation. A dramatic change of impurity behavior is found in the high power discharges. In the discharges with lower NBI heating power, impurity accumulation has been always observed in a specific density (plasma collisionality) range. However, the high power discharges reveal strong suppression of impurity accumulation over the entire density range and a new operational regime without impurity accumulation is found in steady state discharges. Such a drastic change of impurity behavior is caused by the increase in ion temperature gradient and carbon Mach number due to higher NBI heating power. The carbon density profile structure in the high power discharges has been analyzed by CXS measurements and several strong correlations are seen between R/L_{nc} and various plasma parameters. The carbon density profile becomes hollow with increasing the carbon Mach number and toroidal rotation gradient. The carbon peaking also decreases with increasing the

ion temperature gradient, which is closely connected with turbulence.

Momentum transport experiments with changing the NBI torque input provide a more convincing result in the impurity transport. A remarkable change of carbon density in the core plasma is observed by switching the direction of NBI torque input with almost the same NBI heating power. The co-injection beam leads to a hollow profile of carbon density and the counter-injection beam a peaked carbon density profile. In this discharge, there is a big change in the toroidal rotation velocity in the core plasma though the plasma temperatures remain almost unchanged. The carbon density gradient strongly depends on the NBI torque input and the strong co-injection results in an extremely hollow profile of carbon density, which is equivalent to that of 'impurity hole' in high ion temperature modes. In this experimental database, a clear correlation between R/L_{nc} and carbon Mach number is observed in a wide range of the Mach number, which extends up to 0.2. The similar correlation is also seen between R/L_{nc} and toroidal rotation gradient, which increases up to around 4. It can be said that the toroidal rotation plays an important role in the impurity transport.

The high power discharges with net zero torque input (balanced NBI injection) are very useful for investigating the effect of ion temperature gradient on impurity transport, since the toroidal rotation is so small and there is no significant correlation between R/L_{nc} and the rotation parameters. A distinct correlation is observed between R/L_{nc} and the ion temperature gradient and the carbon density profile becomes hollow with increasing the ion temperature gradient. It can be concluded that the ion temperature gradient also contributes to the strong outward convection in the suppression of impurity accumulation.

The strong suppression of impurity accumulation cannot be explained only by neoclassical theory, which predicts a negative radial electric field and inward impurity flux for high Z impurities. In fact, the simulation code DKES/PENTA, which is recently extended with momentum conservation between multi-species particles, indicates that the radial electric field is negative and the impurity flux is inward. Although the neoclassical impurity transport can be modified by an external torque input, it seems to be difficult to produce a drastic modification of neoclassical impurity flux because the Mach-one conditions are needed. One of most probable candidates for the suppression of impurity accumulation is turbulent impurity transport including toroidal rotation effect, which has been investigated in tokamak plasmas. The strong correlations between R/L_{nc} and plasma parameters such as toroidal rotation (its radial gradient) and ion temperature gradient are qualitatively consistent with our experimental results and the theoretical predictions for tokamak plasmas. However, the impurity transport simulation for helical plasmas with an external torque input would be required in future, including neoclassical and turbulent transport.

Acknowledgments

The authors are grateful to the LHD team for their excellent cooperation and to the device engineering group of the LHD for maintaining good operating conditions. The authors are also highly grateful to Dr. D.A. Spong (Oak Ridge National Institute) for providing DKES/PENTA code and to Dr. M. Sato (NIFS) for calculating impurity flux. This work is supported by the budget for the LHD project (NIFSULRR702).

References

[1] Iiyoshi A. et al., Nucl. Fusion **39** (1999) 1245
[2] Pedersen T. S. et al., Nucl. Fusion **55 (**2015) 126001
[3] Nakamura Y. et al., Nucl. Fusion **43** (2003) 219
[4] Nakamura Y. et al., Nucl. Fusion **46** (2006) 714

[5] Mutoh T. et al., Nucl. Fusion **53** (2013) 063017
[6] Kasahara H. et al., Phys. Plasma **21** (2014) 061505
[7] Nakamura Y. et al., Nuclear Materials and Energy, to be published
[8] Nakamura Y. et al., Plasma Phys. Control. Fusion **44** (2002) 2121
[9] Tamura N. et al., Plasma Phys. Control. Fusion **45** (2003) 27
[10] Sudo S. et al., Plasma Phys. Control. Fusion **55** (2013) 095014
[11] Burhenn R. et al., Nucl. Fusion **49** (2009) 065005
[12] Nakamura Y. et al., Plasma Phys. Control. Fusion **56** (2014) 075014
[13] Kobayashi M. et al., Nucl. Fusion **53** (2013) 033011
[14] Kobayashi M. et al., Nucl. Fusion **55** (2015) 104021
[15] Feng Y. et al., Nucl. Fusion **46** (2006) 807
[16] Feng Y. et al., Plasma Phys. Control. Fusion **53** (2011) 024009
[17] Yoshinuma M. et al., Nucl. Fusion **49** (2009) 062002
[18] Ida K. et al., Phys. Plasma **16** (2009) 056111
[19] Yoshinuma M. et al., Nucl. Fusion **55** (2015) 083017
[20] Nagaoka K. et al., Nucl. Fusion **51** (2011) 083022
[21] Spong D. A., Phys. Plasma **12** (2005) 056114
[22] Burrell K. H., Ohkawa T., Wong S. K., Phys. Rev. Lett. **47** (1981) 511
[23] Stacey W. M., Phys. Plasma **16** (2001) 158
[24] Camenen, Y., et al., Phys. Plasma **16** (2009) 012503
[25] Angioni C. et al., Nucl. Fusion **51** (2011) 023006
[26] Casson E. J. et al., Nucl. Fusion **53** (2013) 063026
[27] Nakata M. et al., Plasma Phys. Control. Fusion **58** (2016) 074008
[28] Yoshinuma M. et al., Nucl. Fusion **49** (2009) 075036